Biosensors and Bioelectronics 49 (2013) 236–242

Contents lists available at SciVerse ScienceDirect

Biosensors and Bioelectronics

journal homepage: www.elsevier.com/locate/bios

A label-free DNA hairpin biosensor for colorimetric detection of target with suitable functional DNA partners

Ji Nie, De-Wen Zhang, Cai Tie, Ying-Lin Zhou*, Xin-Xiang Zhang*

Beijing National Laboratory for Molecular Sciences (BNLMS), Key Laboratory of Bioorganic Chemistry and Molecular Engineering, College of Chemistry and Molecular Engineering, Peking University, Beijing 100871, China

ARTICLE INFO

Article history:
Received 11 February 2013
Received in revised form
5 May 2013
Accepted 19 May 2013
Available online 25 May 2013

Keywords:
Hairpin
Sequence design
Aptamer
DNAzyme
Cocaine

ABSTRACT

The combination of aptamer and peroxidase-mimicking DNAzyme within a hairpin structure can form a functional DNA probe. The activities of both aptamer (as biorecognition element) and DNAzyme (as signal amplification element) are blocked via base pairing in the hairpin structure. The presence of target triggers the opening of the hairpin to form target/aptamer complex and releases G-quadruplex sequence which can generate amplified colorimetric signals. In this work, we elaborated a universal and simple procedure to design an efficient and sensitive hairpin probe with suitable functional DNA partners. A fill-in-the-blank process was developed for sequence design, and two key points including the pretreatment of the hairpin probe and the selection of suitable signal transducer sequence were proved to enhance the detection sensitivity. Cocaine was chosen as a model target for a proof of concept. A series of hairpins with different numbers of base pairs in the stem region were prepared. Hairpin-C10 with ten base pairs was screened out and a lowest detectable cocaine concentration of 5 μM by colorimetry was obtained. The proposed functional DNA hairpin showed good selectivity and satisfactory analysis in spiked biologic fluid. The whole "mix-and-measure" detection based on DNA hairpin without the need of immobilization and labeling was indicated to be time and labor saving. The strategy has potential to be transplanted into more smart hairpins toward other targets for general application in bioanalytical chemistry.

1. Introduction

Functional DNAs, including aptamers, DNAzymes and aptazymes, are the members of functional nucleic acid family. Functional DNA biosensors for both small molecule and biomacromolecule have long been developed. Aptamers (Ellington and Szostak, 1990), which were elicited by systematic evolution of ligands by exponential enrichment (SELEX) (Tuerk and Gold, 1990), can specifically interact with their targets as general recognition platforms to establish aptasensors. As a kind of interesting biocatalysts, DNAzymes, playing the roles to be either signal readouts or recognition elements, are also widely used to construct biosensors (Breaker and Joyce, 1994; Robertson and Joyce, 1990). G-quadruplex, which is generated from repetitive G-rich structure motifs, can form G-quadruplex/hemin complexes with hemin and perform peroxidase-like activity (Cheng et al., 2009; Willner et al., 2008). Theoretically, any methods based on horseradish peroxidase (HRP) amplification can be transplanted into G-quadruplex/hemin system, such as colorimetry (Du et al., 2011; Jia et al., 2011), chemiluminescence (Zhou et al., 2012a) and electrochemistry (Pelossof et al., 2010). Therefore, there is growing interest in using DNAzyme as a tag with catalytic activity to amplify label-free biosensing events for a broad range of targets via diverse sensing modes (Liu et al., 2009).

DNA hairpin structures have been enormously reported to analyze different targets such as small drug molecules (Huang et al., 2011), biomarkers (Farjami et al., 2011) and oncogene fragments (Wang et al., 2011). The most universal DNA hairpins are molecular beacons (MBs), which are labeled with both fluorophores and quenchers on DNA ends (Wang et al., 2009). Both the unique stem-loop structure and fluorophore–quencher pair guarantee flexible signal switching of MB in the presence of target. Besides designing aptamer sequence included MB, complete and incomplete G-quadruplex sequences are also encoded into hairpin for signal transduction and amplification. Strand displacement (Fu et al., 2010; Zhou et al., 2012b), target induced switching of DNA conformation (Zheng et al., 2012) and DNA ligase catalyzed nick repairing (He et al., 2012) were used to release caged complete G-quadruplex sequence to develop biosensors via catalytic activity of DNAzyme. For incomplete G-quadruplex sequence, the routine thought is to incorporate the small pieces into completion. Shimron et al. (2011) designed the autonomous cross-opening of the two hairpins, including partly peroxidase-mimicking DNAzyme sequence in caged, to form DNAzyme nanowires for BRCA1 oncogene determination.

* Corresponding authors. Tel.: +8 610 6275 4112; fax: +8 610 6275 4680.
E-mail addresses: zhouyl@pku.edu.cn (Y.-L. Zhou), zxx@pku.edu.cn (X.-X. Zhang).

0956-5663/$ - see front matter © 2013 Elsevier B.V. All rights reserved.
http://dx.doi.org/10.1016/j.bios.2013.05.020

Willner et al. (2008) opened up a new biosensing mode based on aptamer-DNAzyme hairpins for analysis of adenosine monophosphate and lysozyme via DNAzyme catalyzing 2,2′-azino-bis (3-ethylbenzothiazoline-6-sulfonic acid) colorimetric system (Teller et al., 2009). The interaction between the analyte and the loop region of smart hairpin (the main part of aptamer sequence) caused the stem region broken and the release of G-quadruplex domain which was previously caged by base pairing in stem structure. The hairpin probe showed obvious advantages over analogous fluorophore–quencher MB. They also developed the electrochemical biosensor by immobilizing this hairpin on an electrode using peroxidase-mimicking DNAzyme as electrocatalyst (Pelossof et al., 2010). Similar hairpin biosensors for Ochratoxin A (Yang et al., 2012) and human IFN-γ (Zhang et al., 2012) were established via colorimetry and electrochemistry, individually.

A large number of biosensors were based on immobilization or labeling for target trapping and signal transduction. Complicated design, expensive labeling, delicate enzyme or tedious treatments were required, which limited their development for on-site, affordable and rapid point-of-care quantitative analysis. It compels us to seek for the sensing mode to realize a simple "mix-and-measure" assay, which might play important roles in drug abusing characterization, medical diagnostics and modern healthcare. The combination of aptamer and peroxidase-mimicking DNAzyme into a choreographed single strand DNA hairpin structure can meet the above demands. However, for different targets with diverse functional DNA partners, hairpin redesigns were needed. If a foolproof modularization program is developed to construct this kind of hairpin biosensor, all problems will be readily solved. Herein, we demonstrated the universal procedure of how to design a smart functional DNA hairpin as follows. Straightening up the idea, what to do first is sequence design via completing a fill-in-the-blank. A series of hairpins with different numbers of base pairs in the stem region were prepared to search for the optimal sequence structure, which performed sensitive triggering event and the relative low background. After achieving the optimal hairpin, two key points were involved: annealing to obtain stable hairpin with consummate stem duplex; choosing suitable signal transducer sequence with high catalytic activity to improve sensitivity. Cocaine, an addictive stimulant drug for central nervous system, was selected as a proof of concept. According to the above protocols, hairpin-C10 with ten base pairs was screened out, which showed a better sensitivity to cocaine than others. The functional DNA hairpin sensor was successfully applied to detect cocaine in spiked human serum.

2. Experimental

2.1. Reagents and apparatus

All hairpin DNAs were synthesized by Sangon Biological Engineering Technology & Services Co., Ltd. (Shanghai, China) and had the following sequences. (The boldface portion is the DNAzyme sequence EAD2, the italic portion is the DNAzyme sequence PS2.M, and the underlined portion is the anti-cocaine aptamer sequence).

Name	Sequences (5' to 3')
Hairpin-C7	**CTGGGAGGGAGGGAGGGA**TGTGGGAGACAA GGAAAATCCTTCAATGAAGTGGGTCGACATCCC
Hairpin-C9	**CTGGGAGGGAGGGAGGGA**TGTCGGGGAGAC AAGGAAAATCCTTCAATGAAGTGGGTCGACATCCC
Hairpin-C10	**CTGGGAGGGAGGGAGGGA**TGTCGAGGGAGACAA GGAAAATCCTTCAATGAAGTGGGTCGACATCCC
Hairpin-C11	**CTGGGAGGGAGGGAGGGA**TGTCGACGGGAGACA AGGAAAATCCTTCAATGAAGTGGGTCGACATCCC
Hairpin-C12	**CTGGGAGGGAGGGAGGGA**TGTCGACCGGGAGAC AAGGAAAATCCTTCAATGAAGTGGGTCGACATCCC
Hairpin-PS2.M	*GGGTAGGGCGGGTTGGG*TGTCGAGGGAGACAAG GAAAATCCTTCAATGAAGTGGGTCGACACCC

Hemin, magnesium chloride ($MgCl_2$), sodium chloride (NaCl) and potassium chloride (KCl) were purchased from Sigma-Aldrich (St. Louis, MO, USA). Hemin (5 mM) prepared in dimethyl sulfoxide (DMSO) was stored at −20 °C as stock solution. Cocaine hydrochloride was obtained from the National Institute for the Control of Pharmaceutical and Biological Products (Beijing, China). Morphine hydrochloride was obtained from Qinghai pharmaceutical factory (Qinghai, China). TMB · 2HCl (TMB: 4,4′-diamino-3,3′,5,5′-tetramethylbiphenyl) was purchased from Ameresco (USA). Triton X-100 was purchased from Beijing Chemical Reagent Company (Beijing, China). All other reagents were at least of analytical reagent grade and the water used throughout was purified by a Milli-Q system (Bedford, MA, USA).

A number of 96-well plates were purchased from Corning Incorporated (USA). Absorption signals were recorded on Thermo Scientific Multiskan FC Microplate Photometer (USA). Annealing treatment was carried by TC-512 Gradient PCR (TECHNE, UK). The folding and thermodynamic parameters were evaluated using the Oligo-Analyzer program (freely available at *http://www.idtdna.eu/*).

2.2. Colorimetric assay of cocaine using hairpin

All hairpin DNAs were dissolved in working buffer, 25 mM pH 7.4 Tris-HCl buffer (containing 100 mM NaCl, 10 mM KCl, 5 mM $MgCl_2$). The hairpin solution was heated at 95 °C for 5 min and slowly cooled down to 5 °C by PCR machine, then stored at 4 °C. Hemin (100 μM) was freshly prepared in working buffer containing 0.01% Triton X-100. Before use, the hemin solution was diluted to the required concentration with working buffer. For hairpin biosensing of cocaine, equal volume of hairpin (4 μM), hemin (8 μM) and different amount of targets (cocaine) in working buffer were mixed and incubated at 25 °C for 1 h. To check the selectivity of the sensor, morphine was used instead of cocaine. After that, 10 μL of the mixture was dropped into 96-well plate. A 100 μL/well TMB-H_2O_2 solution (0.12 mg/mL TMB · 2HCl, 18 mM H_2O_2, 0.1 M NaH_2PO_4–Na_2HPO_4, pH 6.0) was added to start the chromogenic reaction. Hemin-G-quadruplex DNAzyme can catalyze H_2O_2-mediated oxidation of TMB. Two oxidation products are continuously formed. One is a middle product with blue color (monitored at 620 nm) and the other is an ultimate yellow product (monitored at 450 nm) formed after using strong acids to end the reaction. The kinetic curves were obtained by measuring the absorbance at 620 nm vs. time. After 10 min incubation under 25 °C (avoiding direct light exposure), the reaction was terminated by addition of 50 μL 2 M H_2SO_4. Then the absorbance for quantitation was collected using (A_{450}–A_{620}), a dual wavelengths mode. Or after 5 min of coloration in the dark, the mixtures were terminated for photograph.

2.3. Spiked serum sample treatments

Human serum used in this research was obtained from the local hospital (After the natural coagulation of whole blood, the supernatant obtained by centrifugation was the human serum.). It was subjected to ultrafiltration by loading into centrifugal filtration tubes (MWCO = 10 kDa, Millipore). Different amounts of cocaine, annealing treated hairpin, diluted hemin solution and pretreated human serum were intensively mixed to obtain final spiked serum samples with 20% human serum. The mixture was

used for colorimetric detection following the protocol described in Section 2.2.

3. Results and discussion

3.1. The strategy of designing a smart functional DNA hairpin

As shown in Scheme 1(A), a smart functional DNA hairpin is designed by integrating aptamer as target recognition element and DNAzyme as signal readout element into a single sequence. Their specific functions are blocked by base pairing in a cage, the stem region of hairpin structure. The addition of target can trigger the opening of the hairpin to form target/aptamer complex. Then the presence of hemin results in the self-assembly of G-quadruplex sequence into active DNAzyme. The DNAzyme catalyzes the colorimetric reaction of TMB-H_2O_2 which can provide amplified optical signals for triggering event. As the principle is clear and simple, the most important point of this kind of biosensors is how to design a kind of efficient and sensitive functional DNA hairpin with extensive application.

Cocaine–aptamer interaction was used as a model. In Scheme 1 (B), the loop region is the aptamer of cocaine, and the tail sequence is a G-quadruplex sequence denoted as EAD2. In our design, the duplex structure of stem is the make-or-break issue. Self-assembly of DNAzyme is associated with target triggering event via the stem region. We can adjust the base pair number of the stem duplex to regulate the cage and control the degree of blocking. In order to ensure the sensitive triggering of target, we should reduce the base pair number and weaken the block of both functional elements aptamer and DNAzyme. On the other hand, fewer base pairs might cause DNAzyme to form more easily even without the contribution of target, which would produce a high background signal. If more base pairs are used, it can result in more coaxial stacking interaction to stabilize the secondary structure and reduce the background signal. Although this is a double-edged sword, a simple procedure to seek for the suitable hairpin was put forward. The key point of blocking G-quadruplex sequence of DNAzyme is using complementary base to pair with "G" (guanine). According to the end of G-quadruplex sequence, 5′-end…GGGAGGGA-3′-end, four bases "CCCT" which are highlighted in light blue and labeled in gray box in Scheme 1(B) are chosen to cage the G-quadruplex unit "GGGA". Fixing four base pairs to inhibit peroxidase activity, all that remains is to choose suitable base pair number to block the activity of aptamer. An interesting case in this sequence design is that each time the stem region is lengthened by one base pair, the aptamer-based loop is shortened by one base. As longer loop may more easily bind to the target, it somehow acts in the same direction that is favored by a shorter stem domain. Namely, both the stem domain and the loop domain in the hairpin show effects on the same orientation in target triggering event.

Through doing a fill-in-the-blank (the region of green box in Scheme 1(B)), we designed a series of hairpins with different base pairs, whose numbers were from 7 to 12. The sequence of a hairpin with eight base pairs was "**TGGGAGGGAGGGAGGGA**TG TCGGGAGACAAGGAAAATCCTTCAATGAAGTGGGTCGACATCCC" (5′ to 3′) according to our design principle. In order to keep eight base pairs, we had to add 5′-end …-TGTC-…3′-end in the stem to block the aptamer sequence "ACAG". However, DNA structure tends to keep the thermodynamically stable conformation. The "G" at the beginning of aptamer sequence which was next to "TGTC" would form base pairing with "C" (cytosine) beside "ACAG", thus resulting in an additional complementary "G–C" next to eight base pairs, which finally formed nine base pairs. Due to this reason, we could not obtain a hairpin with eight base pairs obeying our design principle. So, hairpin C-8 was not mentioned in our discussion. The secondary structures and free energy of the five hairpins were evaluated by the Oligo-Analyzer program. As the base pair number increases from seven to twelve, it is found that the free energy values are −7.22 kcal/mol, −11.1 kcal/mol, −12.16 kcal/mol, −14.48 kcal/mol, −16.64 kcal/mol, respectively.

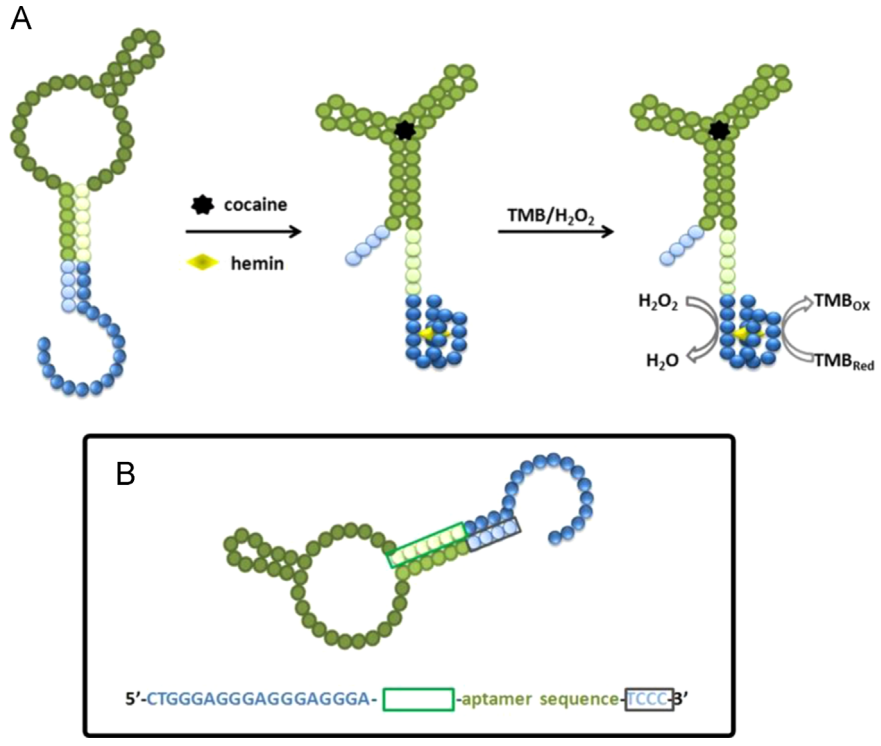

Scheme 1. (A) Principle of smart functional DNA hairpin for target biosensing; (B) secondary structure of hairpin for sensor design (hairpin-C10 for cocaine was showed as a model).

These theoretical data further support the stability of well-formed hairpin structure is related to the complementary state of stem duplex. With the supplementary of software simulation, we tested these hairpins by colorimetric assay. The result illustrated in Fig. 1 was coincided with our hypothesis above. Fewer base pairs led to the high background signal and only high concentration targets could cause obvious signal switching, which might be due that the superiority to open hairpin was covered by the high background signal from easily formed DNAzyme. In contrast, due to the higher thermodynamic stability, more complementary sequence reduced the background signal effectively. The highly stable hairpin was also against high concentration target, and even 10 mM cocaine just generated a slight signal increase. We find that hairpin-C10 performed sensitive signal responses to a wide range of target concentrations from micromole to millimole. Thus, hairpin-C10 was chosen as the optimal hairpin sequence under our experimental conditions.

Two key points to improve the sensing capability of hairpin sequence were obtained from the fill-in-the-blank process. The first is that we have to guarantee the designed sequence to form perfect hairpin structure, which is the premise of achieving ideal sensing performance. DNA denaturation was carried out by heating DNA solution at 95 °C for several minutes. Then slow annealing (the cooling rate was 0.02 °C/s) was operated to allow the stretched sequence to form thermodynamically stable hairpin structure with consummate stem duplex (Li et al., 2011). Comparison between annealed and unheated DNA hairpin was carried out (Fig. S1). Annealed DNA sequence with as low as 10 μM cocaine could cause remarkable signal increase. With unheated DNA, no less than 1 mM target was needed to observe obvious signal change. Slow annealing from high temperature is illustrated to be helpful for hairpin formation. It is reasonable to assume that slow annealing from high temperature is an indispensable step to pledge the perfect hairpin structure, and then improve sensitivity of the assay. The second is choosing suitable DNAzyme sequence with high catalytic activity. A DNAzyme with prominent peroxidase activity can bring out magnifying effect more effective and reliable. Based on the relevant reference (Cheng et al., 2009), EAD2 was selected instead of general used PS2.M (Teller et al., 2009; Zhang et al., 2012). These two DNAzymes were investigated as signal transduction elements in hairpin. At 3′-end of PS2.M, the G-quadruplex unit was GGG, thus three bases CCC were set to block DNAzyme activity. In order to make the two kinds of hairpins at comparable scales, we designed six bases to cage the aptamer sequence in hairpin-PS2.M, which was same to hairpin-C10 with EAD2 sequence. As shown in Fig. S2, when 1 mM cocaine was added, the signal increase obtained by hairpin-C10 (using EAD2) was nine times higher than that using hairpin-PS2.M. It indicates the importance of choosing suitable signal transducer sequence, which can improve sensing capability of functional DNA hairpin.

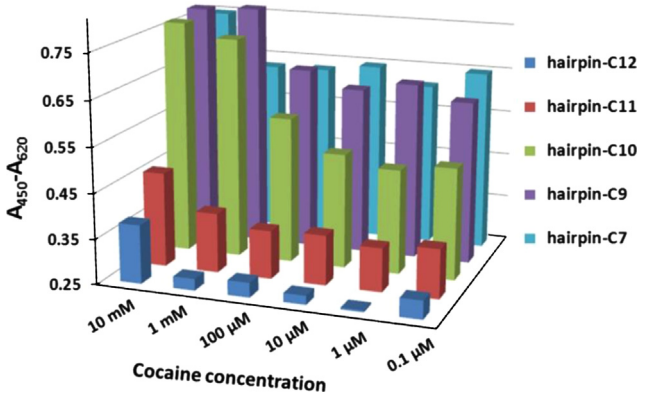

Fig. 1. Colorimetric responses of hairpins with different numbers of base pairs (hairpin-C7, hairpin-C9, hairpin-C10, hairpin-C11, hairpin-C12) in the presence of 0.1 μM, 1 μM, 10 μM, 100 μM, 1 mM, and 10 mM cocaine. SD (standard deviation) <0.027, $n=3$.

3.2. *The performance of the smart functional DNA hairpin of cocaine*

Using the selected hairpin-C10, we investigated the performance of this kind of smart hairpin for cocaine detection based on the principle mentioned above. Without hairpin-C10, hemin did not cause interference as no color change was observed (Fig. 2A).

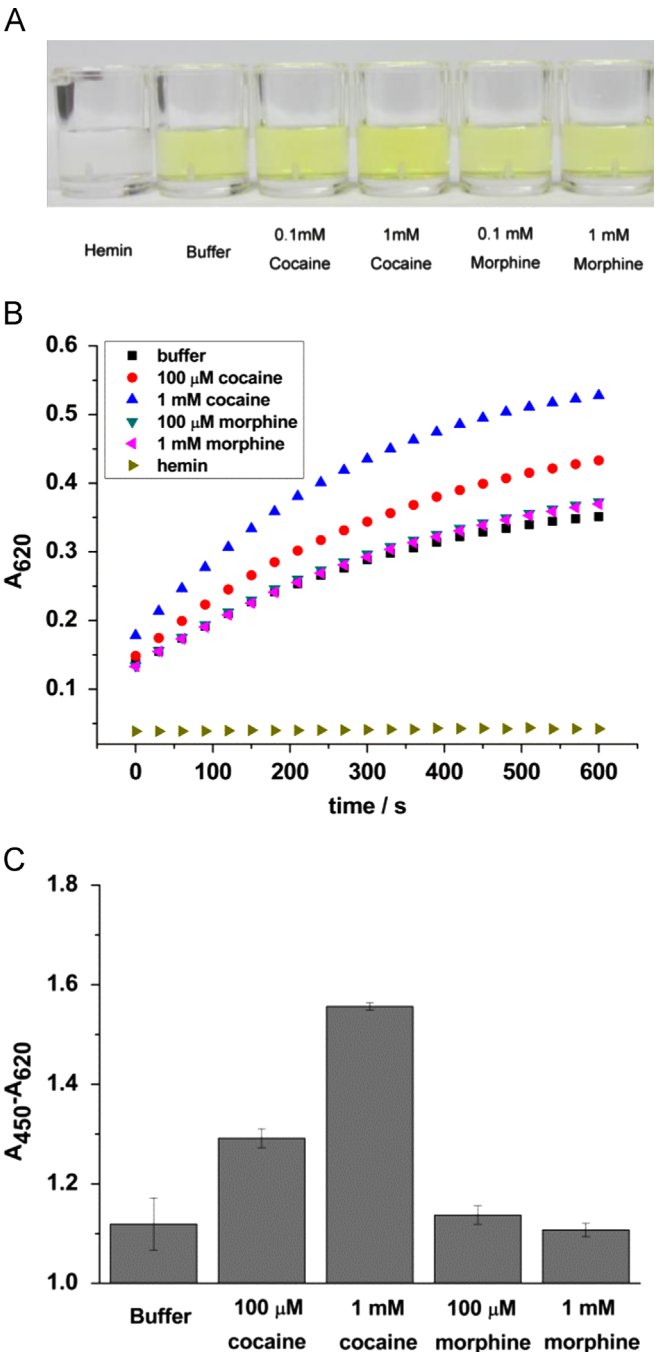

Fig. 2. Selectivity analysis of the DNA hairpin biosensor: (A) The photograph after terminating the reaction with 5 min coloration; (B) the kinetic curves measuring the absorbance at 620 nm vs. time during the 10 min chromogenic reaction; (C) colorimetric responses (A_{450}–A_{620}) after terminating the reaction with 10 min coloration. The control experiments were performed using hemin only (1 mM cocaine was added without hairpin) and different concentrations of cocaine or morphine (0 μM, 100 μM, 1 mM) with hairpin. Error bars: SD, $n=3$.

Both hemin and G-quadruplex sequence were needed to form DNAzyme, and one could not provide peroxidase activity without the other. In the simultaneous presence of hairpin-C10 and hemin, the time-dependent absorbance (A_{620}) along with coloration process and terminated signals ($\triangle(A_{450}–A_{620})$) changed apparently with different concentrations of target cocaine (Fig. 2B and C). In the Fig. 2A, the color changes depend upon the concentrations of cocaine which can be discriminated by the naked eye. The result was consistent with the mechanism that more target molecules opened more hairpins which would lead to form more DNAzymes.

Two control experiments were operated to ensure that the colorimetric signals obtained were due to the trigger of cocaine to open the hairpin stem region, namely, the formation of both cocaine/aptamer complex and G-quadruplex/hemin complex. First, morphine was analyzed instead of cocaine following the same protocol. Only slight signal changes were recorded in the presence of 100 μM or 1 mM morphine. Even 1 mM morphine caused one tenth signal switching of 100 μM cocaine. It demonstrated that the smart hairpin sensor was highly specific to target cocaine, which was benefit from the specific stem-loop structure and affinity recognition of aptamer to target. Two random sequences were used to replace hairpin C-10 to interact with cocaine to do another control experiment. Random I was a sequence which had no related functional sequences. Random II was a sequence without anti-cocaine aptamer region but containing G-rich region. As shown in Fig. S3, only hairpin-C10 shows good performance to cocaine (Fig. S3C and D). Random II containing G-rich region can bind with hemin and show slight catalytic activity which leads to pale yellow (Fig. S3E and F). However, the signals in the absence and presence of cocaine show scarcely any difference. Fig. S3G, H, A and B show no significant difference. The phenomenon indicated that random sequences would not cause signal interference. The above control experiment validated that the formation of both aptamer/target complex and DNAzyme furnished the basis of quantitative analysis of the hairpin aptasensor.

3.3. The optimization of the experimental conditions

A series of optimization experiments were investigated based on the selected hairpin C-10. Incubation time among hairpin, hemin and cocaine was an important factor. The background signal was intensified together with the colorimetric response with the increase of incubation time (Fig. 3A). It is believed that there existed a chemical equilibrium between hemin and hairpin. If enough time were provided, hemin would open the stem region and form DNAzyme. As there was a competition between cocaine opening event and hemin opening event, we should make a decision to guarantee target trigger event to occupy an absolutely dominant position. As shown in Fig. 3A, the incubation time was optimized to 1 h, which ensured the most hairpin release was caused by the formation of aptamer/target complex.

The presence of hemin is necessary to form peroxidase-mimicking DNAzyme. The concentration of hemin would affect the formation of DNAzyme. What is more, excess hemin can promote the trigger equilibrium without target cocaine, which might lead to the high background and weaken the signal change. To analyze the influences of hemin, signal responses caused by different ratios of hemin: hairpin were investigated. And from the measurements presented in Fig. 3B, the ratio of 2:1 was selected to be a preferable condition.

The concentration of hairpin directly determines the generation of colorimetric signal. In the chemical equilibrium among hairpin, cocaine and hemin, if we increased the concentration of any one, the equilibrium would be promoted to open a higher proportion of hairpins. Using 1 mM cocaine as shooters, we optimized the hairpin concentration via recording the kinetic signal increase at 620 nm vs time. As shown in Fig. S4A, both the colorimetric signals in the absence and presence of cocaine are increased with the increase of the hairpin concentration. The increase of hairpin concentration can promote the chemical equilibrium to form more hairpin/cocaine/hemin triplex. At the same time, more hairpins inevitably lead to the higher background signal due to the formation of hairpin/hemin. Signal change (A_{620} (in the presence of 1 mM cocaine)–A_{620} (in the absence of cocaine) vs time was illustrated in Fig. S4B, which clearly demonstrated that 4 μM hairpin generated remarkable signal responses and reached a plateau after about 10 min (the absorbance response recorded at 10 min was slightly higher than that adopting 5 μM hairpin). Thus, the optimized hairpin concentration was 4 μM.

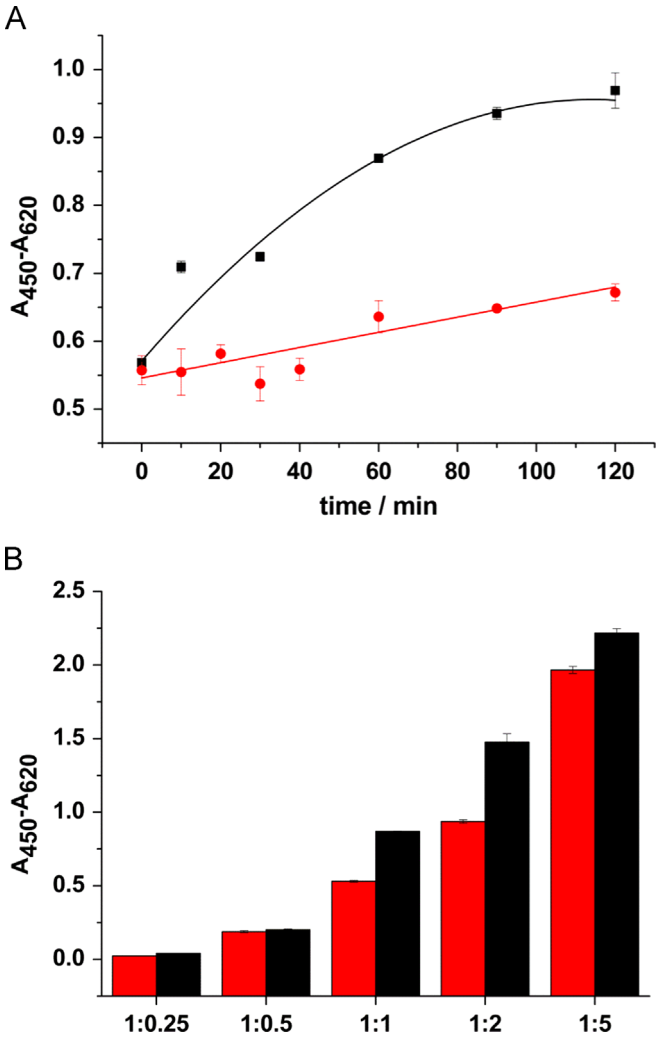

Fig. 3. (A) Colorimetric responses of the hairpin sensor at the different incubation time in the absence (red line) and presence (black line) of 1 mM cocaine. Experimental conditions: hairpin concentration and hemin concentration were fixed to be 4 μM and 8 μM, respectively. Error bars: SD, $n=3$; (B) colorimetric responses of the hairpin sensor with different hemin/hairpin ratios in the absence (red bar) and presence (black bar) of 1 mM cocaine. Experimental conditions: hairpin concentration was fixed to be 4 μM, and hemin concentration was changed to be 1 μM, 2 μM, 4 μM, 8 μM and 20 μM, respectively. Error bars: SD, $n=3$. (For interpretation of the references to color in this figure legend, the reader is referred to the web version of this article.)

3.4. Colorimetric biosensing for cocaine detection

The quantitative performance of our hairpin aptasensor based on peroxidase-mimicking DNAzyme amplification was investigated. Under optimal conditions mentioned above, cocaine samples of different concentrations were mixed with annealed hairpin and

hemin to trigger the whole secondary structure changes. Based on the TMB-H_2O_2 colorimetric detection, kinetic curves monitoring at 620 nm (Fig. 4A) and the absorption values $\triangle(A_{450}–A_{620})$ after termination reaction (Fig. 4B) were recorded in the presence of different cocaine concentrations. The signal responses $\triangle(A_{450}–A_{620})$ increased with the concentration of the added cocaine from 0 μM to 1000 μM, which agreed with the principle that more shooters (cocaine) triggered more hairpin and formed more DNAzyme. The signal increase arrived plateau with 1 mM cocaine, which illustrated the saturation of the hairpin biosensor was reached. As shown in the corresponding calibration curve ranging from 0 μM to 1000 μM, 5 μM is the lowest detectable concentration of cocaine. It should be noted that the dissociation constant of the cocaine/aptamer complex was identified as 5 μM (Stojanovic et al., 2000). As limited by the low affinity capacity of target and aptamer, the sensitivity of relevant biosensor was restricted. Our assay based on hairpin structure is shown to be similar to or even better than many previous homogenous colorimetric assay based on cocaine–aptamer specific affinity interaction (Elbaz et al., 2008; Stojanovic and Landry, 2002; Xia et al., 2010; Zhang et al., 2008). In our homogenous colorimetric assay, the whole "mix-and-measure" procedure can be completed in 1 h without complicated operation, such as separation and immobilization.

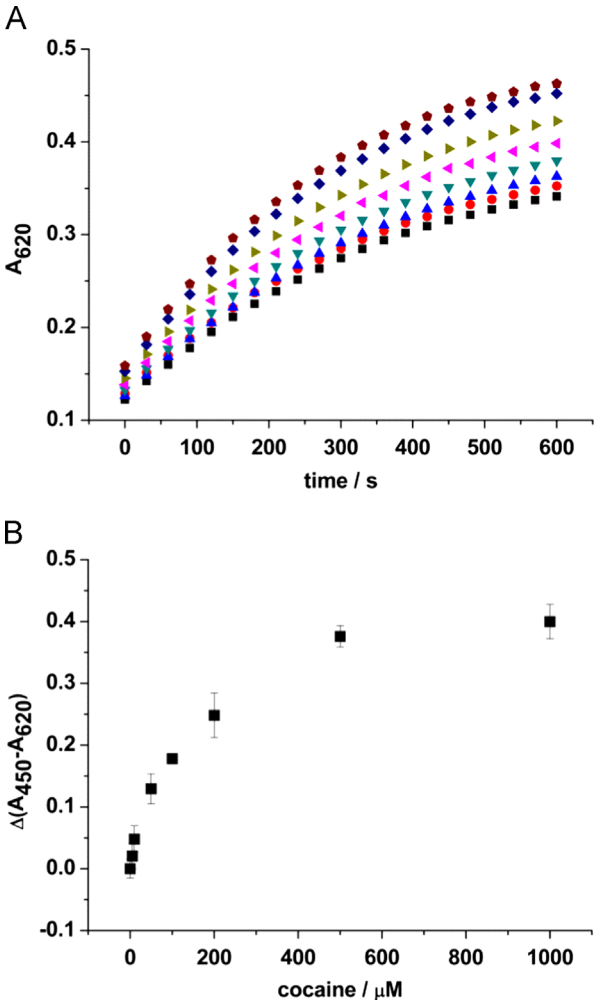

Fig. 4. (A) Time-dependent absorbance changes at A_{620} during the 10 min chromogenic reaction in the presence of different cocaine concentrations. The cocaine concentrations corresponding to curves from bottom to top were 0 μM, 5 μM, 10 μM, 50 μM, 100 μM, 200 μM, 500 μM, 1000 μM, respectively; (B) calibration curve of signal responses $\triangle(A_{450}–A_{620})$ vs. cocaine concentrations. Signal responses were obtained via monitoring dual wavelengths after termination reaction. The experiment was performed under optimal conditions. Error bars: SD, $n=3$.

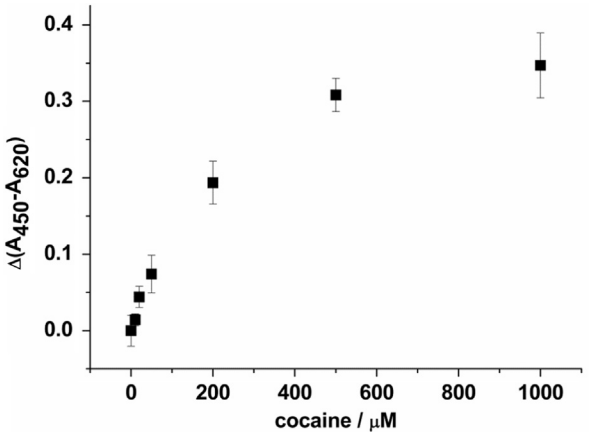

Fig. 5. Calibration curve for cocaine in 20% human serum matrix. The experiment was performed under optimal conditions. Error bars: SD, $n=3$.

The use of high-throughput microplate can realize the analysis of multiple samples simultaneously with the relevant operation time of per sample shortened to be only minutes.

3.5. Application of the hairpin in spiked human serum

We investigated the performance of our hairpin sensing system with complex sample matrix, spiked human serum. The presence of hairpin, hemin and different concentrations of cocaine in 20% (v/v) human serum (sterile-filtered through 10 kDa filter) yielded different responses via DNAzyme catalysis which was also monitored by $\triangle(A_{450}–A_{620})$. A calibration curve for cocaine detection in 20% human serum matrix was demonstrated in Fig. 5. It showed slight signal suppression in human serum when compared with the protocol discribed above in Tris-HCl buffer. The phenomenon might be ascribed to the degradation of the hairpin functional nucleic acid in serum matrix, which led to less ideal hairpin structure and the decrease of response. Even with the signal suppressions, the dynamic range from 10 μM to 1000 μM was achieved. It indicates that our smart functional DNA hairpin has good performance in complex serum matrix and the potential application in the practical samples.

4. Conclusion

In conclusion, we explained the paradigm of how to design a label-free smart functional DNA hairpin biosensor. As cocaine was chosen to be the model molecule, the signal response ranging from 5 μM to 1000 μM was achieved by the functional DNA hairpin biosensor with high selectivity. Even under complex background human serum, the sensor can detect as low as 10 μM cocaine. The whole colorimetric analysis procedure can be completed within 1 h without any complicated operation. While high-throughput microplate is used, multiple samples can be tested simultaneously with the relative handling time per sample shortened to be only minute timescale. The sensitivity of the biosensor limited by the affinity between aptamer and its target is the most critical barrier for its further application. To overcome the limitation for more demand further, more effective amplification should be introduced based on flexible sequence design to realize target recycling or other nucleic acid techniques, such as rolling circle amplification and hybridization chain reaction. We hope that the simple and rapid "mix-and measure" strategy demonstrated here has the potential to open new opportunities for bioanalysis and medicine monitoring.

Acknowledgment

This work was supported by the National Natural Science Foundation of China (No 20805002, 21275009, 30890142, 20975007) and the Scientific Research Foundation for the Returned Overseas Chinese Scholars, MOE. China.

Appendix A. Supporting information

Supplementary data associated with this article can be found in the online version at http://dx.doi.org/10.1016/j.bios.2013.05.020.

References

Breaker, R.R., Joyce, G.F., 1994. Chemistry & Biology 1 (4), 223–229.
Cheng, X., Liu, X., Bing, T., Cao, Z., Shangguan, D., 2009. Biochemistry 48 (33), 7817–7823.
Du, Y., Li, B., Guo, S., Zhou, Z., Zhou, M., Wang, E., Dong, S., 2011. Analyst 136 (3), 493–497.
Elbaz, J., Shlyahovsky, B., Li, D., Willner, I., 2008. ChemBioChem 9 (2), 232–239.
Ellington, A.D., Szostak, J.W., 1990. Nature 346 (6287), 818–822.
Farjami, E., Clima, L., Gothelf, K., Ferapontova, E.E., 2011. Analytical Chemistry 83 (5), 1594–1602.
Fu, R., Li, T., Lee, S.S., Park, H.G., 2010. Analytical Chemistry 83 (2), 494–500.
He, K., Li, W., Nie, Z., Huang, Y., Liu, Z., Nie, L., Yao, S., 2012. Chemistry—A European Journal 18 (13), 3992–3999.
Huang, J., Chen, Y., Yang, L., Zhu, Z., Zhu, G., Yang, X., Wang, K., Tan, W., 2011. Biosensors and Bioelectronics 28 (1), 450–453.
Jia, S.-M., Liu, X.-F., Li, P., Kong, D.-M., Shen, H.-X., 2011. Biosensors and Bioelectronics 27 (1), 148–152.
Li, T., Zhang, L., Ai, J., Dong, S., Wang, E., 2011. ACS Nano 5 (8), 6334–6338.
Liu, J., Cao, Z., Lu, Y., 2009. Chemical Reviews 109 (5), 1948–1998.
Pelossof, G., Tel-Vered, R., Elbaz, J., Willner, I., 2010. Analytical Chemistry 82 (11), 4396–4402.
Robertson, D.L., Joyce, G.F., 1990. Nature 344 (6265), 467–468.
Shimron, S., Wang, F., Orbach, R., Willner, I., 2011. Analytical Chemistry 84 (2), 1042–1048.
Stojanovic, M.N., de Prada, P., Landry, D.W., 2000. Journal of the American Chemical Society 122 (46), 11547–11548.
Stojanovic, M.N., Landry, D.W., 2002. Journal of the American Chemical Society 124 (33), 9678–9679.
Teller, C., Shimron, S., Willner, I., 2009. Analytical Chemistry 81 (21), 9114–9119.
Tuerk, C., Gold, L., 1990. Science 249 (4968), 505–510.
Wang, F., Elbaz, J., Orbach, R., Magen, N., Willner, I., 2011. Journal of the American Chemical Society 133 (43), 17149–17151.
Wang, K., Tang, Z., Yang, C.J., Kim, Y., Fang, X., Li, W., Wu, Y., Medley, C.D., Cao, Z., Li, J., Colon, P., Lin, H., Tan, W., 2009. Angewandte Chemie International Edition 48 (5), 856–870.
Willner, I., Shlyahovsky, B., Zayats, M., Willner, B., 2008. Chemical Society Reviews 37 (6), 1153–1165.
Xia, F., Zuo, X., Yang, R., Xiao, Y., Kang, D., Vallée-Bélisle, A., Gong, X., Yuen, J.D., Hsu, B.B.Y., Heeger, A.J., Plaxco, K.W., 2010. Proceedings of the National Academy of Sciences 107 (24), 10837–10841.
Yang, C., Lates, V., Prieto-Simón, B., Marty, J.-L., Yang, X., 2012. Biosensors and Bioelectronics 32 (1), 208–212.
Zhang, H., Jiang, B., Xiang, Y., Chai, Y., Yuan, R., 2012. Analyst 137 (4), 1020–1023.
Zhang, J., Wang, L., Pan, D., Song, S., Boey, F.Y.C., Zhang, H., Fan, C., 2008. Small 4 (8), 1196–1200.
Zheng, A.-X., Li, J., Wang, J.-R., Song, X.-R., Chen, G.-N., Yang, H.-H., 2012. Chemical Communications 48 (25), 3112–3114.
Zhou, M., Liu, Y., Tu, Y., Tao, G., Yan, J., 2012a. Biosensors and Bioelectronics 35 (1), 489–492.
Zhou, Z., Du, Y., Zhang, L., Dong, S., 2012b. Biosensors and Bioelectronics 34 (1), 100–105.